

## Crystal and Magnetic Structures of the Layer Compound $\text{TiMnF}_4$

P. Nuñez<sup>1</sup>), A. Tressaud, J. Grannec and P. Hagenmuller

Talence (France), Laboratoire de Chimie du Solide du CNRS, Université de Bordeaux I

W. Massa and D. Babel

Marburg, Fachbereich Chemie der Philipps-Universität und Wissenschaftliches Zentrum für Materialwissenschaften

A. Boireau and J. L. Soubeyroux

Grenoble (France), Institut Laue-Langevin

Received June 25th, 1991.

**Abstract.** The crystal structure and the magnetic properties of the fluoromanganate(III)  $\text{TiMnF}_4$  have been investigated. The structure has been refined down to  $R/\text{wR}$  of 0.057/0.043 in the monoclinic  $I2/a$  space group with the unit cell constants  $a = 539.7(2)$  pm;  $b = 544.1(2)$  pm;  $c = 1248.4(5)$  pm;  $\beta = 90.19(3)^\circ$  ( $Z = 4$ ).  $\text{TiMnF}_4$  is characterized by a layer structure formed of  $\text{MnF}_6$  octahedra sharing their four equatorial corners. Within each octahedron the Mn—F distances range from 178 pm to 215 pm. The intralayer magnetic interaction ( $J/\text{k}$ ) has been

evaluated to be approximately  $-0.45$  K by fitting the experimental susceptibility in the 10–300 K range using the quadratic layer Heisenberg model. A 3D-antiferromagnetic ordering occurs at  $T_N = 4.2(5)$  K. The magnetic cell corresponds to the nuclear one but with a primitive symmetry. The magnetic structure has been refined down to  $R = 0.058$  in the  $P2'/a'$  magnetic group. The  $\text{Mn}^{III}$  moments are colinear to the  $b$ -axis and show antiparallel ordering within the layers.

## Kristall- und magnetische Struktur von $\text{TiMnF}_4$ , einer Verbindung mit Schichtstruktur

**Inhaltsübersicht.** Die Kristallstruktur und die magnetischen Eigenschaften des Fluoromanganates(III)  $\text{TiMnF}_4$  wurden untersucht. Die Struktur wurde in der monoklinen Raumgruppe  $I2/a$ , Elementarzelle mit  $a = 539,7(2)$ ;  $b = 544,1(2)$ ;  $c = 1248,4(5)$  pm,  $\beta = 90,19(3)^\circ$  ( $Z = 4$ ) auf  $R/\text{wR}$  0,057/0,043 verfeinert.  $\text{TiMnF}_4$  zeigt eine Schichtstruktur, die durch Eckenverknüpfung von  $\text{MnF}_6$ -Oktaedern über ihre vier äquatorialen Ecken gebildet wird. Die Mn—F-Abstände innerhalb des Oktaeders liegen im Bereich von 178 bis 215 pm. Die magnetische Austauschenergie ( $J/\text{k}$ ) innerhalb der Schicht wurde durch Anpassung der experimentellen Suszeptibilitätsdaten im

Temperaturbereich von 10–300 K auf der Basis des Heisenbergmodells für quadratische Schichten zu  $-0,45$  K bestimmt. Dreidimensionale antiferromagnetische Ordnung tritt bei 4,2(5) K ein. Die magnetische Zelle entspricht der kristallographischen, jedoch mit primitivem Translationsgitter. Die magnetische Struktur wurde auf  $R = 0,058$  in der magnetischen Raumgruppe  $P2'/a'$  verfeinert. Die magnetischen Momente an  $\text{Mn}^{III}$  sind colinear zur  $b$ -Achse und zeigen antiparallele Ordnung innerhalb der Schichten.

**Key words:** Thallium tetrafluoromanganate(III),  $\text{TiMnF}_4$ ; crystal structure; magnetic structure

### Introduction

Many manganese(III) fluorides are known to exhibit chains or layers of corner-sharing octahedra. In addition

a structural distortion generally occurs, which is associated to the strong Jahn-Teller effect of  $\text{Mn}^{III}$  ( $3\text{d}^4$ ) due to its high spin configuration.

Several types of materials appeared to be very good models for one- or two-dimensional magnetic systems. Papers dealing with magnetic properties of  $\text{Mn}^{III}$  fluorides

<sup>1</sup>) Permanent address: Departamento de Química Inorgánica, Universidad de La Laguna, 38200 Tenerife/Spain.

built of chains of trans-[MnF<sub>4</sub>F<sub>2/2</sub>] and/or trans[MnF<sub>2</sub>F<sub>2/2</sub>(H<sub>2</sub>O)<sub>2</sub>] units have been published [1–3].

On the other hand AMnF<sub>4</sub> (A=K, Rb, Cs, NH<sub>4</sub>) phases have been described as layer structures deriving from the TlAlF<sub>4</sub>-type [4, 5]. The distorted (MnF<sub>6</sub>) octahedra are connected by four equatorial vertices. More recently CsMnF<sub>4</sub> has been thoroughly investigated [7]. It is of particular interest as it is a characteristic example of a two-dimensional ferromagnet. It crystallizes in the tetragonal P4/n space group and exhibits antiferrodistortive ordering of elongated (MnF<sub>6</sub>) octahedra. In good agreement with the Goodenough-Kanamori rules for d<sup>4</sup>-d<sup>4</sup>  $\sigma$ -interactions, ferromagnetism has been confirmed by neutron diffraction: the Curie temperature was found to be T<sub>C</sub> = 18.9 K; the magnetic moment was 4.04 BM.

By earlier magnetic measurements [4] a transition from a ferro- to an antiferromagnetic behavior was detected for cations smaller than Cs<sup>+</sup> (A=Rb<sup>+</sup>, NH<sub>4</sub><sup>+</sup> or K<sup>+</sup>). Thus the investigation of an intermediate member of this series such as TlMnF<sub>4</sub> seemed to be worthwhile.

Spectroscopic properties of TlMnF<sub>4</sub> have been previously mentioned but the lattice constants have only been deduced from X-ray powder patterns [4].

In the present research we describe both crystal structure of TlMnF<sub>4</sub> determined by single-crystal X-ray diffraction and magnetic structure obtained from powder neutron diffraction patterns at low temperature. We have also investigated the powder magnetic properties.

## Experimental

**1. Synthesis.** Mn<sub>2</sub>O<sub>3</sub>, prepared by decomposition of manganese(II) nitrate [6], was dissolved in aqueous hydrofluoric acid (40%). Separately a Tl<sup>+</sup> solution was obtained by dissolving Tl<sub>2</sub>CO<sub>3</sub> in a similar 40% HF solution. The two solutions were mixed in such a way that the Tl : Mn molar ratio was 1 : 1. The resulting solution was maintained in a covered polyethylene vessel for several days at about 50°C. Small dark-brown crystals were grown in those conditions.

**2. Elemental analysis.** Elemental analysis was carried out at CNRS Service Central d'Analyse. The metallic element concentration was determined using a multielement atomic absorption spectrometer and fluoride ions were titrated using an anion-selective electrode. The concentrations are the following:

- observed: Mn(16.40), Tl(60.80), F(21.51)%
- calculated for TlMnF<sub>4</sub> composition: Mn(16.38), Tl(60.35), F(22.67)%.

**3. Structural investigation.** A small brown crystal was selected for X-ray diffraction measurements on a four circle-diffractometer (Enraf-Nonius) using MoK $\alpha$ -radiation and a graphite monochromator. The lattice constants were refined from 25 high-angle reflections. The main experimental crystallographic data are listed in Table 1.

**Table 1** Experimental crystallographic data for TlMnF<sub>4</sub>

Crystal data	
Formula	TlMnF <sub>4</sub>
Molecular weight	335.308
Crystal dimensions	approx. 0.1×0.06×0.05 mm <sup>3</sup>
Absorption	$\mu = 455 \text{ cm}^{-1}$ , empirical correction
Space group	I2/a, Z = 4
Pseudo symmetry	Imam
Lattice constants (MoK $\alpha$ )	$a = 539.7(2) \text{ pm}$ $b = 544.1(2) \text{ pm}$ $c = 1248.4(5) \text{ pm}$ $\beta = 90.19(3)^\circ$
Temperature	293 K
Voluminal mass	$\rho = 6.07 \text{ g cm}^{-3}$
Data collection	
Diffractometer	4-circle, CAD4 (Enraf-Nonius)
Radiation	Mo-K $\alpha$ , graphite monochromator
Scanning-type	$\omega$ -scanning
Scanning width	(1.5 + 0.35 tg $\theta$ )° and 25% on the left and right side of a reflection for background determinations
Measuring range	2° < $\theta$ < 30°, $\pm h$ , $+k$ , $+l$ and $h k \bar{l}$
Reflections Total	888
Independent	506; 423 > 5 $\sigma(F_o)$
Computing	
Structure determination	Patterson methods (SHELXS-86 [8b])
Refinement	minimizing $\Sigma(\Delta F)^2$ (SHELX 76 [8a])
Scattering factors	extracted from [10]
Anomalous dispersion	extracted from [11]
Extinction coefficient	$\varepsilon = 3.5 \times 10^{-8}$ [8a]
R-values	$R = 0.057$ , $wR = 0.043$ (31 parameters) [ $w = 1/\sigma^2(F_o)$ ]

Lorentz-polarization correction was made and an empirical absorption correction (Psi-scans) was applied ( $\mu = 455 \text{ cm}^{-1}$ ). 423 reflections were considered with  $F_o > 5\sigma(F_o)$ .

The crystal showed only small deviations from an orthorhombic symmetry Imam. This result explains why in an earlier powder work [4] the true monoclinic space group I2/a was not detected.

The structure was determined from a Patterson map and from subsequent Fourier syntheses and could be refined with

**Table 2** Atomic coordinates and anisotropic thermal parameters [10<sup>-20</sup> m<sup>2</sup>] for TlMnF<sub>4</sub> (space group I2/a)

Atom	x	y	z	U <sub>11</sub>	U <sub>22</sub>	U <sub>33</sub>	U <sub>23</sub>	U <sub>13</sub>	U <sub>12</sub>
Mn	0.25	0.75	0.25	0.011(2)	0.010(2)	0.010(2)	0.000(2)	-0.002(2)	0.002(2)
F1	0.277(2)	0.661(2)	0.114(1)	0.034(7)	0.026(5)	0.016(7)	-0.005(5)	0.007(7)	0.002(6)
F2	0.471(2)	1.066(2)	0.214(1)	0.018(7)	0.023(6)	0.048(11)	0.003(6)	-0.014(8)	-0.016(5)
Tl	0.25	0.2332(3)	0.0	0.0307(8)	0.0204(7)	0.030(1)	0.0	-0.0032(7)	0.0

anisotropic temperature factors for each atom down to a final  $R = 0.057$  and  $wR = 0.043$ .<sup>2)</sup> Final position and thermal parameters are reported in Table 2.

**4. Magnetic measurements.** Magnetic measurements were performed on powder sample with a SQUID magnetometer in the 2–300 K temperature range. The applied field ranged from 0 to 5 T. A correction for diamagnetic contribution was taken into account.

**5. Neutron diffraction measurements.** Neutron diffraction experiments were carried out at the high flux reactor of the Institut Laue-Langevin in Grenoble using the D1B powder diffractometer which is equipped with a large position-sensitive detector (PSD). Diffractograms were recorded with the incident wavelength  $\lambda = 252.2$  pm. The powder sample was set in a vanadium container and a  $4^\circ \leq 2\theta \leq 84^\circ$  angular domain has been covered. Patterns were registered between 1.5 and 200 K using a liquid helium cryostat. Crystallographic and magnetic structures were determined using the Rietveld profile refinement technique with the Young program [12]. The nuclear scattering lengths and the magnetic form factors were taken from reference [13] and [14] respectively.

## Results and Discussion

### 1 Crystal structure

$\text{TiMnF}_4$  has a layer structure deriving from the  $\text{TiAlF}_4$ -type, i.e. formed by  $[\text{MnF}_6]$  octahedra sharing their four equatorial corners (Fig. 1). As for  $\text{CsMnF}_4$  the Jahn-Teller effect of the  $d^4$  high-spin configuration leads to a strong elongation of the octahedra (Table 3). The directions of the long axes ( $\text{Mn—F2} = 215$  pm) constitute an antiferrodistortive arrangement within the layers. The shorter  $\text{Mn—F}$  distances correspond to bridging bonds ( $\text{Mn'}—\text{F2} = 186$  pm) and very short terminal bonds ( $\text{Mn—F1} = 178$  pm).

The layers differ from those of  $\text{CsMnF}_4$  by the bridge angles  $\text{Mn—F—Mn}$  which decrease from  $161.9^\circ$  for  $\text{CsMnF}_4$  to  $146.5^\circ$  for  $\text{TiMnF}_4$ , and by the puckering type. The layers alternate with the 12-coordinated  $\text{Ti}^{+}$  ions (see. Fig. 6, Table 3).

We have recently investigated the structural and magnetic properties of the hydrates  $\text{Ti}[\text{MnF}_4(\text{H}_2\text{O})]$  and  $\text{Ti}_2[\text{MnF}_5] \cdot \text{H}_2\text{O}$  [3], both showing octahedral trans-chain structures.

### 2 Magnetic behavior

The temperature dependence of the reciprocal molar susceptibility for powder samples is plotted in Fig. 2. In the investigated temperature range a linear variation is ob-

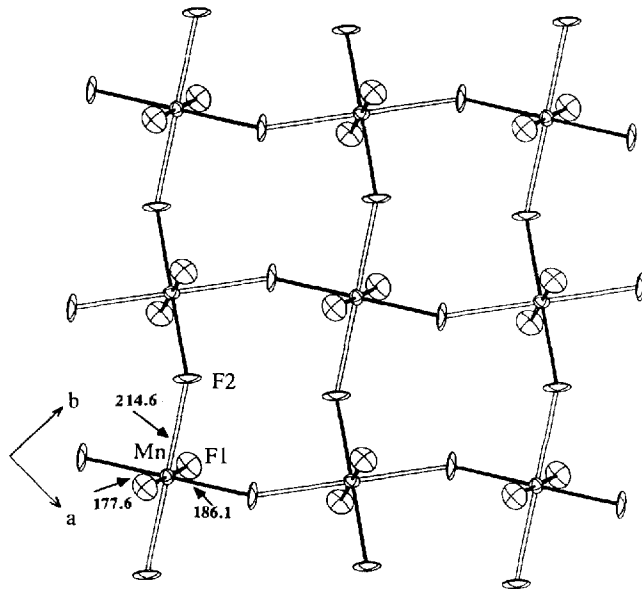


Fig. 1 Arrangement of  $\text{MnF}_6$  octahedra in  $\text{TiMnF}_4$ : (a, b) plane; white double lines: elongated axes;  $\text{Mn—F}$  distances in pm (ORTEP drawing [9]: thermal ellipsoids at the 50% probability level)

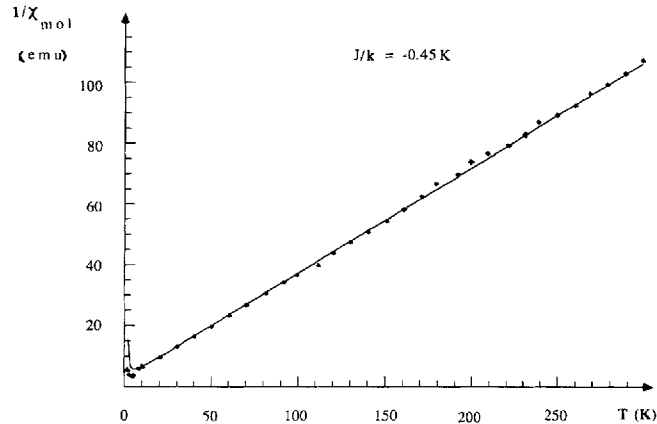


Fig. 2 Temperature dependence of the reciprocal susceptibility of  $\text{TiMnF}_4$

served with a small  $\theta_p$  value of  $-7$  K. The experimental Curie constant ( $C_M = 2.87$ ) is in good agreement with the usual values found for manganese(III) compounds.

The exchange constant between Mn atoms within a plane ( $J/k$ ) has been calculated by fitting the susceptibility data to the quadratic layer Heisenberg antiferromagnetic model as described by Lines [15]. Fitting was based on the following equation:

$$\frac{Ng^2\beta^2}{J_{\chi(T)}} = 3\theta + \sum_{n=1}^{\infty} \frac{C_n}{\theta^{n-1}},$$

where  $\theta = KT/JS(S+1)$ ,  $g$  is the Lande factor,  $N$  the number of spins in the lattice,  $C_n$  are coefficients calculated from the general formalism of ref. [16].

<sup>2)</sup> The structure factor tables have been deposited in the Fachinformationszentrum Karlsruhe, Gesellschaft für wissenschaftlich-technische Information, W-7514 Eggenstein-Leopoldshafen 2, with number CSD-55 897.

This method allowed to fit the broad susceptibility maximum which experimentally characterizes two-dimensional quasi-Heisenberg antiferromagnets. It yielded an intralayer exchange constant:  $J/k = -0.45$  K. The weakness of this value can account for the low value of the 3D-ordering antiferromagnetic temperature (see below).

According to Goodenough-Kanamori rules, an antiferrodistortive ( $MnX_6$ ) octahedra arrangement is generally associated with a ferromagnetic behavior, whereas a ferrodistortive structural arrangement leads to antiferromagnetism. X-ray and neutron diffraction studies on  $CsMnF_4$  seemed to confirm such an assumption: the antiferrodistortive arrangement observed for this material induces a bulk ferromagnetism [5]. On the other hand the magnetic  $J/k$  value obtained for  $TlMnF_4$  at first sight contradicts the above rules:  $TlMnF_4$  exhibits an intralayer antiferromagnetic behavior associated with an antiferrodistortive structural arrangement.

If we compare the layer structure of  $TlMnF_4$  with that of  $CsMnF_4$  we observe actually that the exchange angles  $Mn-F-Mn$  are quite different from each other. In  $TlMnF_4$  this angle is about  $146.5^\circ$ , which corresponds to a deviation from the ideal angle ( $180^\circ$ ) stronger than that of  $CsMnF_4$  ( $161.9^\circ$ ). In such conditions the mixtures of the  $d_{xz}$  and  $d_{yz}$   $Mn^{3+}$  orbitals forming  $\pi$ -bonds with the  $p_x$  and  $p_y$  orbitals of fluorine have to be considered; these couplings which are responsible for antiferromagnetism strongly compete with the  $e_g-p\sigma-e_g$  interactions. This trend is in good agreement with that previously observed in other series of  $Mn^{III}$  fluorides [2].

### 3 Magnetic structure

A neutron diffraction study has been carried out down to 1.34 K (Fig. 3). The study of the temperature dependence of the intensity of some magnetic peaks in the 1.34–20 K temperature range has allowed to determine the 3D-magnetic ordering temperature  $T_N = 4.2(5)$  K (see Fig. 4). The magnetic peaks which appear below  $T_N$  can be indexed in the nuclear cell but with a primitive lattice. The unit cell constants at 1.34 K are the following:  $a = 536.1(2)$  pm;  $b = 539.7(2)$  pm;  $c = 1243.5(3)$  pm;  $\beta = 89.20(1)^\circ$ .

Various magnetic configurations have been tested to fit the observed intensities. The best result, which corresponds to a magnetic R-factor of 0.058, with  $R_{magn} = 100 \times \sum [I_{magn}(\text{obs}) - I_{magn}(\text{calc})] / \sum I_{magn}(\text{obs})$  can be described as follows: in the magnetic cell the magnetic atoms are assigned to two different sites: Mn1 ( $1/4, 3/4, 1/4$ ); Mn2 ( $3/4, 1/4, 3/4$ ).

Magnetic moments of both Mn1 and Mn2 atoms appear to be colinear to the b-axis and antiparallel to each other with a value of  $3.1(3)$  BM. The refined neutron diffraction pattern corresponding to such a hypothesis is given in Fig. 5. The expected value of the resulting magnetic moment is about 3.5 BM for a magnetic ion with  $S = 2$ . However, due to the low value of the Neel tempe-

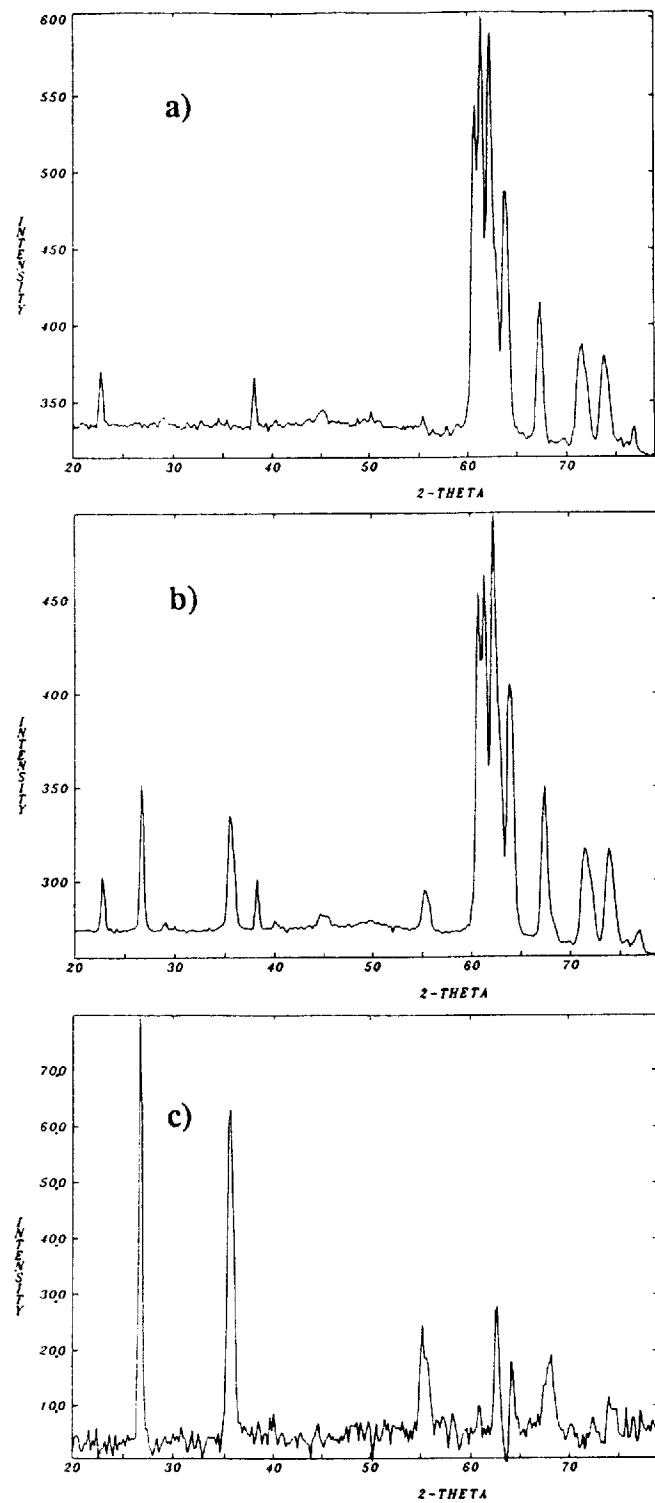


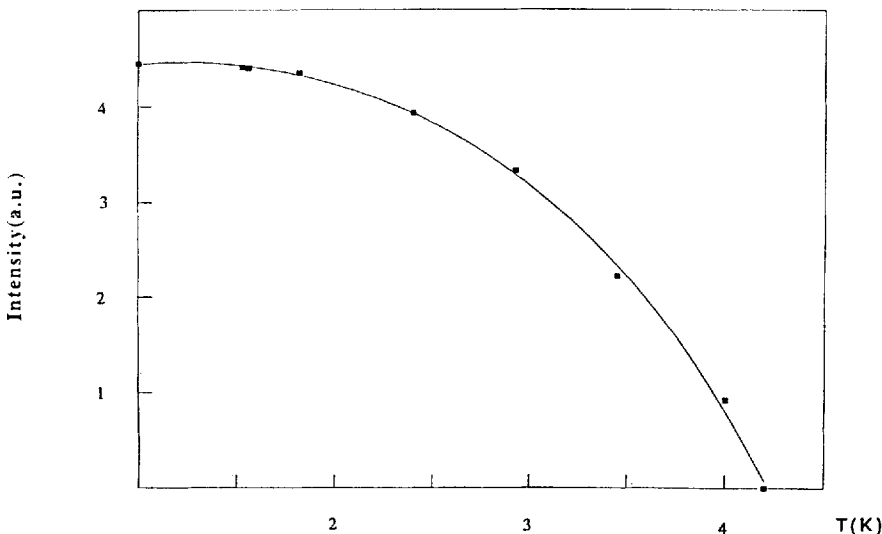
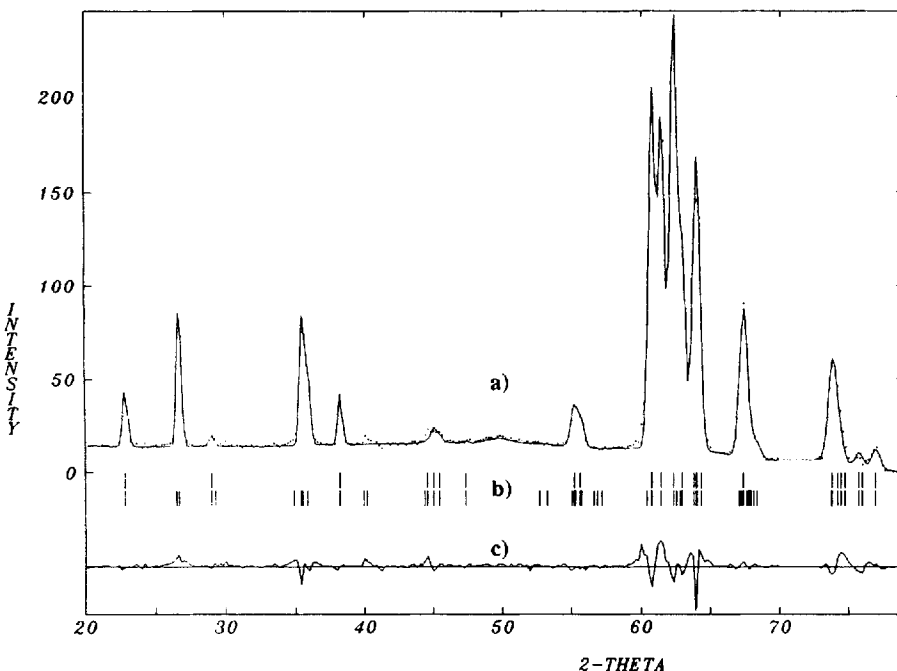
Fig. 3 Experimental neutron diffractograms of  $TlMnF_4$  at  $T = 8$  K<sup>a</sup>),  $T = 1.34$  K<sup>b</sup>) and difference pattern<sup>c</sup>)

rature this difference can be attributed to an incomplete saturation of the moment at 1.34 K. Observed and calculated intensities for such a model are collected in Table 4. We can describe therefore the magnetic structure as formed of  $Mn^{III}$  atoms antiferromagnetically coupled inside

**Table 3** Interatomic distances [pm] and angles [deg] in  $\text{TlMnF}_4$ 

Mn—F1	2×	177.6(10)	Tl—F1,F1 <sup>i</sup> )	2×	273(1)
Mn—F2	2×	186.1(10)	Tl—F1 <sup>j</sup> )	2×	298(1)
Mn <sup>a</sup> )—F2	2×	214.6(10)	Tl—F2 <sup>k</sup> )	2×	307(1)
			Tl—F1 <sup>a</sup> ) <sup>b</sup> )	2×	322(1)
mean Mn—F		192.8	Tl—F1 <sup>k</sup> ) <sup>j</sup> )	2×	342(1)
			Tl—F2 <sup>a</sup> ) <sup>j</sup> )	2×	348(1)
F1—Mn—F2		88.5(5)			
F1—Mn—F2 <sup>b</sup> )		89.2(6)	mean Tl—F		315
F2—Mn—F2 <sup>b</sup> )		88.2(5)			
			in plane:		
Mn—F2—Mn <sup>a</sup> )		146.5(7)	Mn ··· Mn	4×	383.2(2)
			between planes:		
			Mn ··· Mn	2×	624.2(3)

Symmetry operations: <sup>a</sup>) 0.5+x, 1-y, z; <sup>b</sup>) x-0.5, 2-y, z; <sup>c</sup>) 1-x, y-0.5, 0.5-z; <sup>d</sup>) 0.5+x, 2-y, z; <sup>e</sup>) 1-x, -y, -z; <sup>f</sup>) -x, -y, -z; <sup>g</sup>) 1-x, 1-y, -z; <sup>h</sup>) -x, 1-y, -z; <sup>i</sup>) 0.5-x, y, -z; <sup>j</sup>) x-0.5, 1-y, z; <sup>k</sup>) x, y-1, z; <sup>l</sup>) 0.5-x, y-1, -z

**Fig. 4** Temperature dependence of the (100) magnetic peak**Fig. 5** Refined neutron diffraction pattern of  $\text{TlMnF}_4$  at  $T = 1.34 \text{ K}$  [calculated profile intensities (full line) a); positions of nuclear peaks (above) and magnetic peaks (below) b); difference spectrum c)]

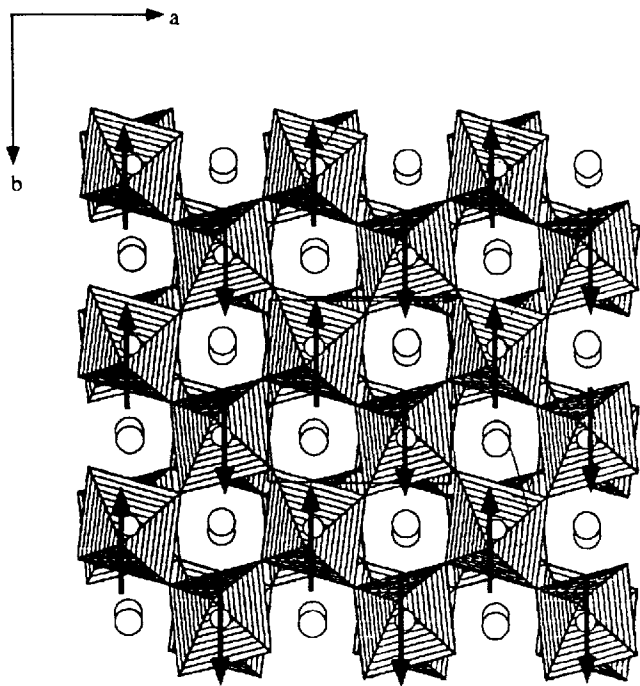


Fig. 6 Magnetic structure of  $\text{TlMnF}_4$

Table 4 Observed and calculated intensities of magnetic reflections for  $\text{TlMnF}_4$  at  $T = 1.34 \text{ K}$

$h \ k \ l$	$I_{\text{calc.}}$	$I_{\text{obs.}}$	$h \ k \ l$	$I_{\text{calc.}}$	$I_{\text{obs.}}$
1 0 0	3264	3716	1 0 4	553	613
1 0 2	1700	1990	1 2 0	161	172
0 1 2	1489	1453	2 1 0	631	701
1 0 2	1686	1723	1 2 2	195	201
1 0 4	562	569	2 1 2	524	539
0 1 4	850	887	1 2 2	197	206
			2 1 2	518	558

a layer and ferromagnetically coupled between two alternating planes with a compensated resulting moment as shown in Fig. 6. This scheme corresponds to the  $\text{P}2'/\text{a}'$  magnetic group.

### Conclusions

The structural and magnetic data obtained for  $\text{TlMnF}_4$  point out the strong influence of the Mn—F—Mn bridging angle on the magnetic couplings: an antiferromagnetic ordering is observed instead of the ferromagnetic behavior which could be expected as a consequence of the antiferrodistortive structural ordering shown in Fig. 1. This result illustrates the competition between  $\sigma$ - and  $\pi$ -superexchange mechanisms for low bridging angles. It con-

firms the previous investigations on the  $\text{Mn}^{III}$  chain compounds  $\text{A}_2\text{MnF}_5 \cdot x\text{H}_2\text{O}$  ( $\text{A}$  = monovalent cation;  $x = 0$  or 1) in which the intrachain antiparallel exchange constant has been shown to decrease strongly with decreasing Mn—F—Mn bridging angles [2]. The small negative values of the intralayer exchange constant ( $J/k = -0.45 \text{ K}$ ) thus gives an indication of the presence of both parallel and antiparallel coupling mechanisms within a layer.

The authors are indebted to J. Darriet for valuable discussions. One of us (PN) thanks the Government of Canary Islands for a grant. This work has been carried out in the scope of an EEC Research Program.

### References

- [1] P. Nuñez, J. Darriet, P. Bukovec, A. Tressaud, P. Hagenmuller: *Mat. Res. Bull.* **22** (1987) 661
- [2] J. Pebler, W. Massa, H. Lass, B. Ziegler: *J. Solid State Chem.* **71** (1987) 87
- [3] P. Nuñez, A. Tressaud, J. Darriet, P. Hagenmuller, F. Hahn, G. Frenzen, W. Massa, D. Babel, A. Boireau, J. L. Soubeyroux: *Inorg. Chem.*, to appear (1992)
- [4] P. Köhler, W. Massa, D. Reinen, B. Hofmann, R. Hoppe: *Z. anorg. allg. Chem.* **446** (1978) 131
- [5] W. Massa, M. Steiner: *J. Solid State Chem.* **32** (1980) 137
- [6] T. E. Moore, M. Ellis, P. E. Selwood: *J. Am. Chem. Soc.* **72** (1950) 856
- [7] W. Massa: *Gesellschaft Deutscher Chemiker, Hauptversammlung*, Bonn 1989, VCH Weinheim, p. 323
- [8] G. M. Sheldrick: a) SHELX-76, Program for Crystal Structure Determination, Cambridge (1976), b) SHELXS-86, Program for Crystal Structure Solution, Göttingen (1986)
- [9] C. K. Johnson: ORTEP, A Fortran Thermal Ellipsoid Plot Program for Crystal Structure Illustrations, Report ORNL-3794, Oak Ridge, USA (1965)
- [10] D. T. Cromer, J. D. Mann: *Acta Crystallogr.* **A24** (1968) 321
- [11] D. T. Cromer, D. Libermann: *J. Chem. Phys.* **53** (1970) 1891
- [12] R. A. Young, D. B. Wiles: *J. Appl. Crystallogr.* **14** (1981) 149
- [13] V. F. Sears: Internal Report AECL-8490 (1984)
- [14] P. J. Brown: "International Tables for Crystallography", vol. C to appear (1992)
- [15] M. E. Lines: *J. Phys. Chem. Solids* **31** (1970) 101
- [16] G. S. Rushbrooke, P. J. Wood: *Mol. Phys.* **1** (1958) 257

Address for correspondence:

Dr. A. Tressaud  
Laboratoire de Chimie du Solide du CNRS, Univ.  
Bordeaux I  
F-33405, Talence Cedex, France